Integrated Fabrication and Magnetic Positioning of Metallic and Polymeric Nanowires Embedded in Thin Epoxy Slabs

Darren J. Lipomi,[†] Filip Ilievski,[†] Benjamin J. Wiley,[†] Parag B. Deotare,[‡] Marko Lončar,[‡] and George M. Whitesides[†,*]

[†]Harvard University, Department of Chemistry and Chemical Biology, 12 Oxford Street, Cambridge, Massachusetts 02138, and [‡]Harvard University, School of Engineering and Applied Sciences, 33 Oxford Street, Cambridge, Massachusetts 02138

This paper describes an integrated approach to the fabrication and positioning of nanowires embedded in thin slabs of polymer. The procedure combines nanoskiving—a technique for the fabrication of nanostructures that uses an ultramicrotome to cut thin slabs of nonmagnetic and ferromagnetic materials embedded in a polymeric matrix[1,2]—with noncontact, magnetic manipulation of the polymeric slabs containing ferromagnetic particles (Figure 1 summarizes the process, which we have named "magnetic mooring"). Magnetic mooring exploits an important characteristic of nanoskiving; that is, after sectioning, the nanostructures remain embedded in thin slabs of polymer, which float on the surface of water. The user can collect the slabs by transferring them to a substrate, along with ~5 μL of water. The water forms a pool on which the slabs float and across whose surface they can be moved using magnetic interactions. As the water evaporates, capillary interactions cause the slabs to adhere to the substrate. In this work, we coembedded Ni strips or powder with the nanowires in order to make the floating slabs (along with the nanostructures they contain) magnetically responsive to the field created by a movable external magnet. The accuracy of registration of the embedded nanostructures with predeposited objects on a substrate was typically 5−25 μm.

Magnetic mooring can form geometries of nanostructures for electronic and photonic applications that would be difficult or impossible to arrange using other techniques. We crossed nanowires of Au, Pd,

ABSTRACT This paper describes a process for the fabrication and positioning of nanowires (of Au, Pd, and conjugated polymers) embedded in thin epoxy slabs. The procedure has four steps: (i) coembedding a thin film of metal or conducting polymer with a thin film of nickel metal (Ni) in epoxy; (ii) sectioning the embedded structures into nanowires with an ultramicrotome ("nanoskiving"); (iii) floating the epoxy sections on a pool of water; and (iv) positioning the sections with an external magnet to a desired location ("magnetic mooring"). As the water evaporates, capillary interactions cause the sections to adhere to the substrate. Both the Ni and epoxy can be etched to generate free-standing metallic nanowires. The average translational deviation in the positioning of two nanowires with respect to each other is 16 ± 13 μm, and the average angular deviation is 3 ± 2°. Successive depositions of nanowires yield the following structures of interest for electronic and photonic applications: electrically continuous junctions of two Au nanowires, two Au nanowires spanned by a poly(3-hexylthiophene) (P3HT) nanowire; single-crystalline Au nanowires that cross; crossbar arrays of Au nanowires; crossbar arrays of Au and Pd nanowires; and a 50 × 50 array of poly(benzimidazobenzophenanthroline ladder) (BBL) nanowires. Single-crystalline Au nanowires can be placed on glass wool fibers or on microfabricated polymeric waveguides, with which the nanowire can be addressed optically.

KEYWORDS: nanoskiving · nanowires · nanofabrication · conjugated polymers · microtome · nanophotonics · nanowire positioning · magnetic positioning

and conjugated polymers, and were able to place individual single-crystalline Au nanowires on dielectric waveguides. The procedure is nonphotolithographic, and requires only methods for the deposition of thin films, an ultramicrotome, a microscope, and a movable stage for positioning. It is compatible with conventional methods of lithography for subsequent electrical or optical characterization. The process provides a way of fabricating, positioning, and integrating nanostructures with each other and with instruments in the laboratory.

BACKGROUND

Positioning Nanoscale Objects. Nanoscience and nanotechnology require methods to address and manipulate nanostructures

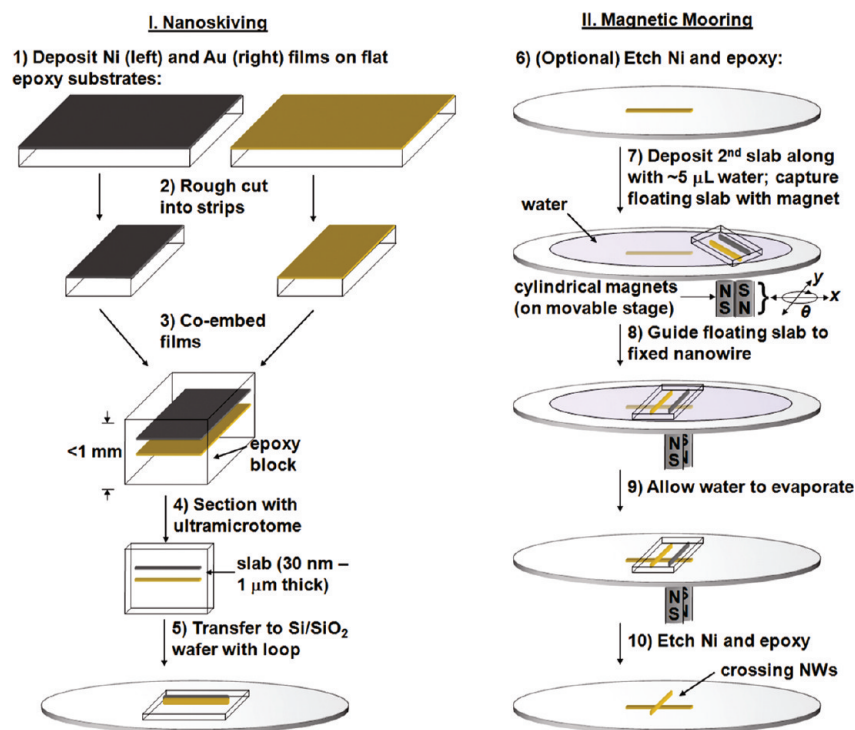*Address correspondence to gwhitesides@gmwgroup.harvard.edu.

Figure 1. Schematic representation of the procedure used for fabrication (I. nanoskiving) and positioning (II. magnetic mooring) of nanowires.

Nanoscience often requires the interactions of multiple structures in close proximity in well-defined geometries, for example, specific structures comprising nanowires, quantum dots, electrodes, waveguides, and other structures in functional forms.[4] The more elements a system has, however, the lower the probability that a desired geometry can be generated by random assembly. Systems in which geometry is important, and of course, any engineering application require methods of fabricating multielement structures that do not rely on chance.

Existing Methods for Positioning Nanowires. Existing methods for positioning nanowires have one of two goals: (i) to align a large number of nanowires over a large area (cm²)[5,6] or (ii) to position individual nanowires one-by-one.

Shear alignment of nanowires suspended in fluids[7] is a common method to fabricate useful geometries of nanowires of several classes of materials.[8−11] Lieber and co-workers have recently extended shear alignment of nanowires to the scale of cm² by suspending and depositing them in bubble-blown films.[12] Brushing suspensions of nanowires over a lithographically patterned substrate creates highly aligned regions of nanowires on exposed areas of the substrate.[13] Alignment of nanowires in a Langmuir−Blodgett trough can form highly anisotropic films that can be cast over large areas.[14] In general, shear alignment is capable of manipulating the orientation of many nanowires at once but with limited control of the position of individual nanowires.

Optical tweezing can manipulate single semiconducting nanowires in a liquid environment with a high theoretical accuracy.[15] Opto-electronic tweezing is a new technique in which an optical signal creates an electrical potential on a photoconductive layer on the bottom of a liquid-filled cell to yield groups of nanowires aligned perpendicular to the substrate in arbitrary locations.[16] Optical methods of manipulation, in general, depend on the size, shape, and composition of the nanostructures, and on the presence of a fluid.

Methods of manipulation by direct contact with scanning probe tips[17] and micromanipulators[18] can provide control over individual nanowires, but are dependent on the size and composition of the nanowires and the topography of the substrate. Electrophoretic alignment of nanowires over prepatterned electrodes has the potential for integration over large areas,[19] but it requires an extensively processed substrate. The pitch of the nanowires, further, may only be as high as that of the spacing between electrodes. Templated elec-

individually and in groups. There are many strategies for fabricating nanostructures and assembling them into useful geometries. Scanning-beam techniques such as electron-beam lithography (EBL) are well-established and can generate nearly arbitrary patterns in resist, which can be transferred to metallic thin films or other materials. Focused-ion-beam (FIB) milling can carve patterns into materials directly and is used extensively in research laboratories for the fabrication of test structures. These techniques, powerful as they are, have high costs, low throughput, limited accessibility to general users, and limited flexibility with respect to the types of substrates they can pattern directly. In this discussion, we focus on structures fabricated through non-lithographic means, and then deposited on a substrate in a desired geometry. This paper uses structures that are one-dimensional[3] (nanowires, nanorods, etc.), but the process we describe would be applicable to other structures or arrays of structures as well.

Nonlithographically generated nanostructures are usually deposited by random assembly. Once deposited, nanostructures arranged by chance in a desired geometry can be addressed lithographically. Alternatively, nanostructures can be deposited on a substrate already bearing lithographically patterned features. A serendipitously positioned nanowire (spanning two electrodes or sitting on an optical waveguide) can then sometimes be addressed. This method proceeds with low yields and provides little control over the orientation of nanostructures.

trodeposition in lithographically defined trenches,[20] or by self-assembled structures of block copolymers,[21] allow integrated fabrication and alignment of structures, but these methods are limited to materials grown electrochemically.

Use of Magnetic Forces in Nanoscience. The use of magnetism to manipulate nanostructures has usually been limited to structures that are themselves magnetic.[22−25] For example, Hangarter *et al*. prepared Au and Bi nanowires capped with Ni and aligned them on magnetic electrodes.[26]

Magnetism is generally regarded as nonharmful to biological systems, at low fields. This characteristic has inspired biomedical applications of magnetic nanoparticles that include attachment to biomolecules[27] and microtubules,[28] actuation of magnetic particles internalized by living cells to promote cell death,[29] and the fabrication of particles that could be localized using magnetic fields for drug delivery.[30]

Combination of magnetic forces with self-assembly provides another method to position small structures. Yellen *et al*. demonstrated the self-assembly of nonmagnetic particles when suspended in a medium containing magnetic particles arranged by a programmable, magnetic substrate.[31] In another example, Lapointe *et al*. suspended Ni nanowires in a bed of nematic liquid crystals, which was patterned into zones in which the molecular orientation (director) pointed in different directions. At equilibrium, the nanowires self-aligned with their long axes parallel to the director. When the authors reoriented nanowires with a magnetic field, the nanowires migrated to a different region of the pattern such that their long axes were again parallel to the director.[32]

We reasoned that any nanowire, including those of nonmagnetic materials, could be manipulated by an external magnet if the wire could be tethered physically to a magnetic particle. For example, Shi *et al*. modified the surfaces of glass fibers with Fe_3O_4 nanoparticles using layer-by-layer assembly and observed the motion of the fiber on the surface of water in the presence of a magnetic field.[33]

Nanoskiving. Nanoskiving is a technique based on sectioning thin structures (*e.g*., films or microplates) with an ultramicrotome.[1] We have used this process to generate nanowires from polymeric thin films formed by spin-coating,[34,35] metallic thin films formed by physical vapor deposition,[36] and chemically grown, single-crystalline microplates.[37] Our laboratory has previously described an approach to orient structures produced by nanoskiving, by stacking successive slabs manually (by hand, with an eyelash, or another tool).[1]

EXPERIMENTAL DESIGN

Our goal was to develop a method to position polymeric slabs containing nanowires on flat or topographically patterned substrates. At its core, this process re-

quired forming thin slabs of polymer that embedded both the nanowires and a sacrificial ferromagnetic material. These slabs, floating on the surface of a pool of water, would be mobile under the influence of an external permanent magnet. As the water evaporated, the polymeric slabs would become docked ("moored") to the substrate in the position fixed by the user. While there are potentially many ways of generating such films, we chose to combine this technique with nanoskiving. Even though nanoskiving is capable of forming several types of nanostructures, all of which would be amenable to positioning by the process we are describing, we focused on nanowires for the following reasons: (i) they are straightforward to fabricate by sectioning thin films or microplates, and thus make good systems with which to characterize this method; (ii) the lines they make in epoxy slabs make them easy to locate using optical microscopy (which would facilitate positioning) and (iii) they are important components of nanoelectronic and nanophotonic devices.[3]

We chose Ni as the sacrificial ferromagnetic material to coembed with the nonmagnetic nanowires in the epoxy matrix. While Ni has a lower magnetic permeability than other ferromagnetic materials (*e.g*., Fe), Ni is mechanically softer. Softer materials are less likely than harder materials to damage the diamond knife we use in the ultramicrotome.

We reasoned that the best geometry of Ni particle with which to embed the nanowires would be a long strip for magnetostatic considerations.[38] An external magnet would magnetically saturate the Ni strip in the long direction. Two separate effects would account for the translational and rotational positioning of the epoxy slabs in the magnetic field. The first effect, maximizing the flux of the field through the Ni strip, would govern the initial capture and translation of the epoxy slab on the pool of water. An epoxy slab, mobile on the surface of the droplet of water, would move over the external magnet until the Ni strip reached the region with the highest flux. The second effect, the torque acting on the magnetic moment of the polarized Ni strip in the external field, would enable rotational alignment. We chose the dimensions of the Ni strips ($l \approx 10^2$ μm and $w \approx 2$ μm) as a compromise between two different goals: (i) maximizing the absolute strength of interaction with an external magnetic field (which is proportional to the volume of the ferromagnetic material) and (ii) minimizing the thickness of the Ni film (a film that is too thick can damage the diamond knife). The thickness of the epoxy slabs became the height of the Ni strips, which constrained that dimension to 100 nm for all experiments in this paper. An alternative method of adding ferromagnetic particles to the epoxy slabs was to mix Ni nanopowder (particle size ≈ 200 nm) into the epoxy prepolymer (2% by mass Ni); this method would be convenient but would sacrifice some control in positioning slabs.

ACSNANO

We designed the experimental apparatus for simplicity. It required a microscope and two stages: the upper stage held the substrate, typically a Si wafer, sitting over a circular hole drilled into the stage with a diameter ($d = 1.5$ in.) smaller than that of the Si wafer ($d = 2$ in.); the lower stage had a movable platform, with three degrees of freedom (x, y, and θ), which supported the magnets (grade N42, NdFeB, cylindrical, $d = 0.125$ in., $l = 0.375$ in.) and enabled translation and rotation of the magnetic field. We assembled six of these magnets into two parallel columns of three magnets each (to increase the height of the magnetic column), with the magnetization of each column pointing in the opposite direction. The top of the dual column of magnets was positioned so that it was <0.5 mm from the bottom of the substrate. The opposite polarization of the top of each of the two magnets magnetized the strips of Ni in the floating slabs and allowed for manipulation of the slabs by translation and rotation of the magnetic field (see the Supporting Information for photographs of the apparatus).

Fabrication. Figure 1 summarizes both phases of the procedure: fabrication (nanoskiving) and positioning (magnetic mooring). We illustrated the process for the simple case of generating crossed Au nanowires, but it is easily amenable to structures of any material that can be fabricated by nanoskiving. We deposited two thin films, one of Ni (2 μm thick) and one of Au (80 nm thick), on flat epoxy substrates by electron-beam evaporation (step 1). Then, using a razor blade, we cut strips (<1 mm × 5 mm) of Ni and Au supported by their epoxy substrates (step 2). We embedded the strips together in epoxy prepolymer (step 3). We sectioned the blocks with the ultramicrotome into epoxy slabs (step 4), which we transferred to the substrate using a metallic loop that suspended the slab by surface tension in a thin film of water (the "Perfect Loop" tool, inner diameter = 2 mm, obtained from Electron Microscopy Sciences; step 5). The substrates used in this work were typically test-grade Si wafers bearing a native layer of SiO_2, cleaned with an air plasma (500 mtorr, 100 W, 30 s). Optionally, selectively etching the epoxy in an air plasma (100 W, 1 Torr, 15 min), and the Ni with a commercial etchant, left behind a free-standing nanowire on the surface (step 6). We transferred a second epoxy slab to the substrate by hand using the Perfect Loop. When touched to the substrate, the loop released the slab along with a droplet of water of ~5 μL, which spread into a pool ~1 cm in diameter (step 7). We captured the floating slab in the magnetic field of the column of magnets mounted on the movable stage. By manipulating the position of the magnets, we guided the second slab over the first nanowire in the desired orientation (a cross, step 8). As the water evaporated, capillary forces caused the slab to adhere to the substrate (step 9). The epoxy and Ni could be etched, as before; this action yielded free-standing, crossing nanowires (step 10).

RESULTS AND DISCUSSION

Thin Epoxy Slabs Containing Nanowires and Ni Particles. Figure 1 shows the preferred method of incorporating Ni particles into epoxy slabs containing nanowires by co-embedding evaporated Ni films. Sectioning 2-μm-thick films of Ni formed strips in the epoxy slabs that enabled manipulation by an external magnet. (Sectioning thinner Ni films (100 nm) provided extensively fractured wires that did not have sufficient volume for capture and manipulation of the slabs by the external magnet.) The alternative method was to make a "magnetic epoxy" by mixing Ni powder into the epoxy prepolymer. Either method of incorporating Ni (strips or powder) into the epoxy provided 100−500 pg of Ni in a typical slab with dimensions $l \approx w \approx 500$ μm, $h = 100$ nm. Figure 2 shows optical micrographs of typical epoxy slabs containing nanowires and Ni particles. The features stand out most clearly under dark field.

Magnetic Manipulation of Thin Epoxy Slabs. We were able to manipulate slabs containing Ni along with metallic and polymeric nanowires with maximum velocities of ~100 μm s⁻¹. It took about 2 min to position each floating slab on the surface of the water. The 5-μL pool of water typically evaporated in 10 min if the stage was heated gently to ~35 °C with a halogen lamp placed 10 cm away. We found that it was more difficult to rotate slabs containing Ni powder than it was to rotate those containing Ni strips; as we rotated the column of permanent magnets, the epoxy slabs bearing Ni powder slipped unpredictably from one equilibrium position to another, though some control was possible. We attribute the difference in the ability to control the position of slabs containing Ni strips and those containing Ni powder to differences in shape of the embedded magnetic particles. The Ni powder consists roughly of spheres, which are weakly interacting with each other and can be magnetized easily in any direction. In contrast, the anisotropic shape of a Ni strip forces the magnetization along the long axis and makes it more difficult to demagnetize than Ni powder by a moving magnetic field. Consequently, the slabs embedded with powder are more difficult to capture and control with an applied field than those containing strips.

Electrical Continuity of Two Crossing Au Nanowires. The first geometry of nanowires that we demonstrated comprised two Au nanowires that crossed at 90°; we then characterized the electrical conductivity of the wires and the junction. On a Si wafer bearing ~300 nm of thermally grown SiO_2, we moored two 100-nm-thick epoxy slabs, which contained one Au nanowire each ($l \approx 200$ μm, $w = 80$ nm, $h = 100$ nm). After positioning, the slabs were heated to 125 °C for ~15 min in an oven to improve adhesion of the epoxy to the substrate. Next, we defined contact pads using a hand-cut conformal stencil mask made of a poly(dimethylsiloxane) (PDMS) membrane (100 μm thick), through which we deposited 50 nm of Au by electron-beam evaporation. Before

characterization, the epoxy matrix was removed by a treatment in an air plasma. While this procedure can be performed at any point, we left the epoxy matrix until the end so that it would provide structural integrity against the conformal PDMS mask, which might otherwise damage free-standing nanowires. We measured the electrical characteristics of the crossing nanowires after removal of the epoxy matrix. We were able to apply up to ± 10 mV without failure of the nanowires; when we increased the bias beyond ± 10 mV, the circuit failed, presumably by melting at a thin area of one of the wires (the crossing region itself remained intact, as determined by scanning electron microscopy). Figure 3a shows the plot of current density vs voltage ($J-V$). In the calculation of current density, we assumed a uniform rectangular cross section of the wires of 80 nm $\times$ 100 nm, which spanned a length of 100 μm, as determined by SEM. The current density was 0.4 of the theoretical maximum based on the conductivity of bulk Au. We attribute the lower effective conductivity to nonuniform cross sections of the wires, a nonconformal junction between them, the graininess of the parent thin films, and possible contamination of organic material between the nanowires.

Au Nanowire Electrodes Spanned by a Conjugated Polymer Nanowire. To demonstrate the ability to mix different types of materials, we generated a system that spanned two Au nanowires with a poly(3-hexylthiophene) (P3HT) nanowire. This geometry could be useful in measuring nanoscale charge transport in optoelectronic polymers and in the fabrication of chemical sensors[39] or field-effect transistors based on single nanowires.[40] Poly(3-hexylthiophene) (which we synthesized using established methods[41]) undergoes an insulator-to-metal transition upon exposure to I_2.[42] We began by depositing two parallel Au nanowires, which were embedded in the same epoxy slab (thickness = 100 nm). We removed 10−20 nm of the epoxy surrounding free Au nanowires by brief etching with an air plasma. We chose not to etch the epoxy completely because occasionally, immersion in water during the mooring step dislodged Au nanowires that were unsupported by epoxy slabs (Au adheres poorly to SiO_2). We fabricated a P3HT nanowire (100 nm $\times$ 100 nm cross section), coembedded with Ni powder in epoxy, and moored it in a position that spanned the 50-μm gap between Au nanowires. We did not remove the epoxy matrix surrounding the P3HT wire, since to do so would have destroyed the P3HT. We deposited contact pads though a stencil mask as described previously. In the absence of I_2, the current of the nanowires at ± 1 V was too low to be detected by our electrometer (Keithley 6430 Femtoammeter). When we placed an I_2 crystal ~ 1 mm away from the P3HT nanowire (uncovered), the conductivity of the P3HT increased within 10 s (the time it took to acquire an $I-V$ plot). Figure 3b shows the conductivity of the nanowire when exposed to I_2 ("doped") and the con-
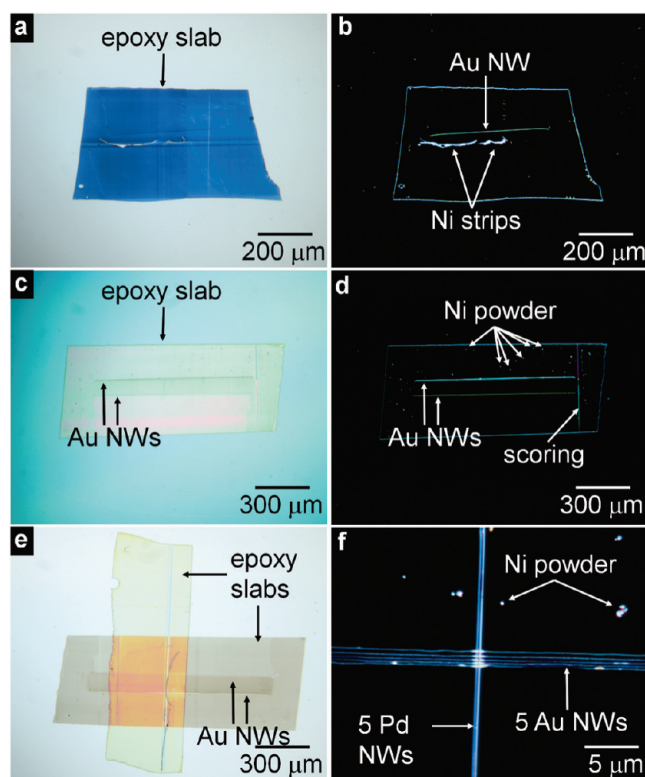
Figure 2. Optical micrographs of epoxy slabs containing nanostructures and sacrificial Ni particles. All slabs are 100 nm thick. (a) An epoxy slab containing an Au NW and strips of Ni; the features stand out in the dark-field image shown in panel b. The Ni strips look damaged because of buckling of the Ni film, possibly due to thermal expansion and contraction of the epoxy substrate during the process of evaporation. (c) An epoxy slab containing two parallel Au nanowires coembedded with Ni nanopowder. The dark-field image (d) shows light scattering off of the nanowires and the powder. The upper Au nanowire appears thicker because the epoxy matrix is delaminated from the Au (the interface scatters light strongly). A defect in the cutting edge of the diamond knife created a line of scoring parallel to the direction of cutting, which stands out under dark field. (e) Two crossing epoxy slabs positioned by mooring. (f) Dark-field image of five parallel Au nanowires crossing five parallel Pd nanowires (the spacing is too small to resolve the Pd nanowires individually). The Au and the Pd nanowires were deposited in single epoxy slabs containing five nanowires each.

ductivity after removal of the I_2 ("undoped"). We did not try to achieve the maximum doping level reported for P3HT.[42] It should be possible to fabricate arrangements of nanowire electrodes for four-terminal measurements; this geometry would allow decoupling of the contact resistance from the true resistance of a nanowire.

Accuracy of Positioning. To determine the accuracy with which we could position and orient nanostructures on top of one another, we formed crosses of single-crystalline Au nanowires (which we obtained by nanoskiving chemically synthesized Au microplates[37]), with the goal of superimposing the center of each nanowire with a crossing angle of 90°. We used Ni strips as the sacrificial ferromagnetic material for this experiment. Figure 4a is an SEM image of two crossing nanowires, which have a center-to-center distance (deviation) of 2.2 μm. The average center-to-center dis-
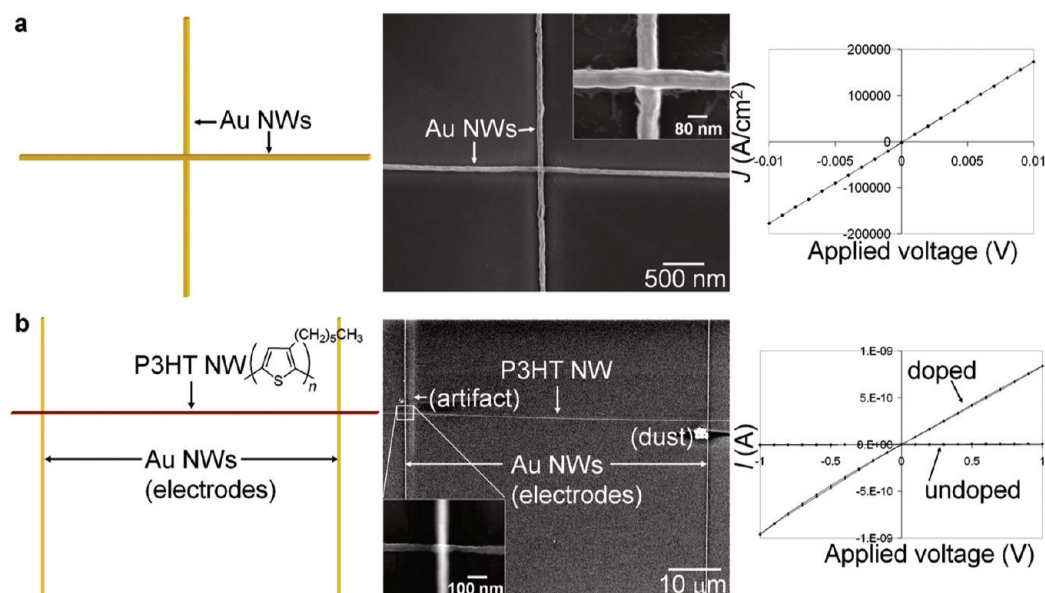
Figure 3. Images of junctions of single nanowires (NWs) fabricated by nanoskiving and magnetic mooring, and demonstration of electrical continuity. (a) Schematic illustration and scanning electron micrograph (SEM) of perpendicular Au nanowires and a plot of current density *vs* voltage ($J-V$) that demonstrates conductivity through the junction. The SEMs in panels a and b were obtained before the deposition of contact pads. (b) Illustration and SEM of parallel Au nanowires separated by 50 μm and spanned by a P3HT nanowire embedded in an epoxy slab. The epoxy was not etched because the air plasma would have destroyed the P3HT. The inset is a close-up of the junction (the Au nanowire is out of focus because the epoxy slab that contains the P3HT nanowire obstructs the electron beam; a particle of dust and a hazy vertical artifact of the image are labeled). The plot of current *vs* voltage ($I-V$) demonstrates that the P3HT increased in conductivity upon exposure to I_2 ("doped"). Upon removal of the I_2, the conductivity of the P3HT nanowire decreased ("undoped").

tance over 10 attempted crossings ($N = 10$) was 16 $\pm$ 13 μm, and the average angular deviation (from perpendicular) was 3 $\pm$ 2°. The Supporting Information contains images of all 10 attempted crossings in the data set. The mooring process is subject to human error; the registration is performed by eye under 95$\times$ magnification and the slabs are manipulated using an analog micromanipulator. There are many possible ways to improve the accuracy. For example, using long nanowires ($>$100 μm) and an eyepiece containing a square grid, it was possible to reduce the average angular deviation to 0.7 $\pm$ 0.5° ($N = 4$). We estimated that the amplitude of vibrations visible in the microscope was 1–5 μm (due to noise, air currents, and other vibrations in the room). The best realizable accuracy depends on the interplay between the floating slab and the receding edge of the drop of water (the interface between the drop of water and the dry substrate). For a clean surface (*e.g.*, a Si wafer or glass slide cleaned with a brief exposure to an air plasma), the water will recede toward the floating slab smoothly as the water evaporates. As the edge of the drop advances toward the floating slab, the slab tends to travel toward the edge, as if sliding downhill. This perturbation is typically $<$10 μm and can be corrected by the user. For a contaminated surface (one that has been left open to the ambient air for a day or more), the drop edge does not recede smoothly. Rather, episodes of abrupt dewetting of the substrate at the drop edge create vibrations that can displace the slab away from its equilib-

rium position by 10 μm or more. The addition of surfactants increases the wettability of the substrate by the water, but leaves residue upon evaporation. The use of solvents with low surface tension in addition to or instead of water could make the process amenable to hydrophobic substrates without contaminating the surface.

Stacking more than two slabs should be possible as well. The only caution is that a predeposited epoxy slab dewets with a different rate than does the SiO_2 substrate. We found that abrupt dewetting of the drop over epoxy slabs attached to the substrate often displaced the floating slab; we obtained the most accurate results by ensuring that the retreating drop edge intersected the floating slab over the SiO_2, rather than over a fixed slab. Any amount of overhang (of the floating slab above the fixed slab) was sufficient to bypass the effect of rapid dewetting over slabs attached to the surface. We have not observed that the magnetic field of the predeposited Ni particles interferes with the mooring process.

Crossbars. Crossbar arrays of long nanowires with spacing between nanowires approximately equal to the widths of the nanowires can be made by nanoskiving and magnetic mooring. We fabricated crossbars of Au (Figure 4b), of Au and Pd (Figure 4c), and a 50 $\times$ 50 square array of the conjugated polymer poly(benzimidazobenzophenanthroline) ladder (BBL, Figure 4d). In each case, the vertical nanowires were fabricated and moored as a group over the horizontal nanowires. We
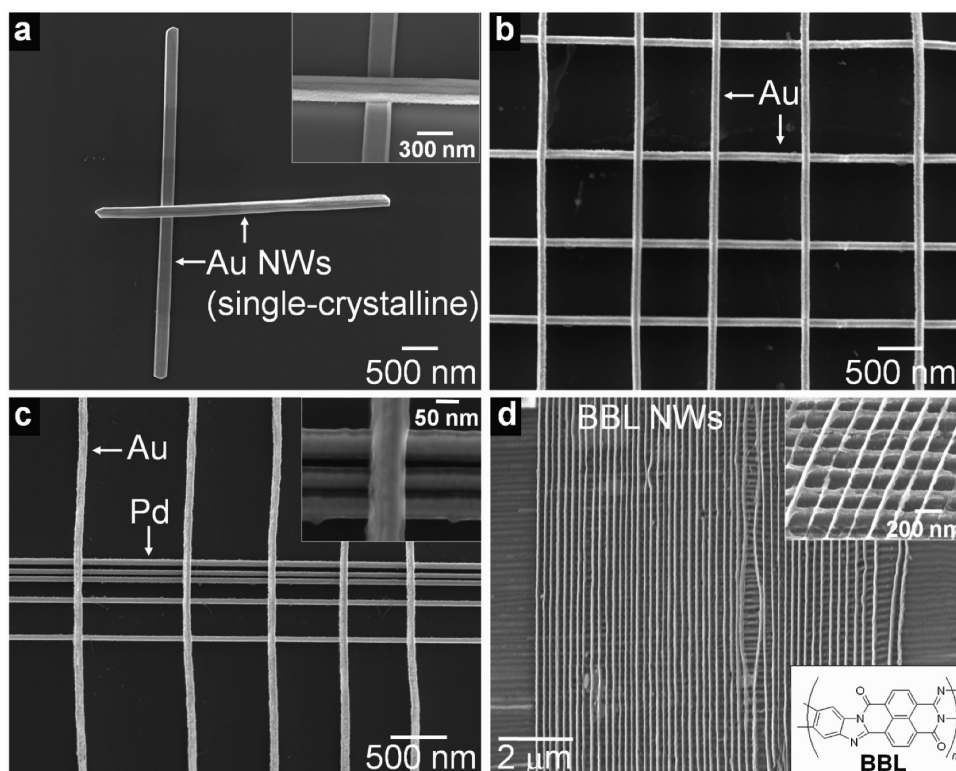
Figure 4. Crossbar structures formed by nanoskiving and magnetic mooring. (a) SEM image of crossing single-crystalline Au nanowires. The vertical nanowire has dimensions of l = 10 μm, w = 300 nm, h = 100 nm; the horizontal nanowire has dimensions of l = 8 μm, w = 290 nm, h = 100 nm. The centers of the nanowires are separated by 2.2 μm, and the long axes deviate from perpendicular by 2.6°. The inset was obtained at a tilt of 45°. **(b)** An array of Au nanowires with dimensions of individual nanowires of w = 80 nm and h = 100 nm. **(c)** An array of Pd nanowires (w = 60 nm, h = 80 nm) crossed by Au nanowires (w = 80 nm, h = 100 nm). **(d)** A 50 × 50 square array of poly(benzimidazobenzophenanthroline ladder) (BBL) nanowires. The pitch is 200 nm. We attribute the defects in which the nanowires diverge, touch, or both to delamination of the thin films from which the nanowires are made, during the sectioning process.

used Ni powder as the sacrificial ferromagnetic material in Figure 4b—d.

Mooring Nanowires onto Topographic Features. We were able to moor nanowires on top of topographic features on a substrate, as long as the pool of water submerged the features during the process of positioning. We deposited a 15-μm-long, single-crystalline Au nanowire on a single fiber of glass wool (Figure 5a), as well as an 8-μm-long nanowire on a 1-cm-long, 10-μm-wide, 2-μm-high, waveguide fabricated by EBL in SU-8, negative-tone resist (Figure 5b).

Scattering from a Nanowire on a Waveguide. To show that light could be coupled into the nanowire by the evanescent field near the surface of a polymer waveguide, we used an optical fiber to couple light into the waveguide and observed scattering from the termini of the nanowire. Figure 5c is a schematic drawing of the arrangement between the nanowire, waveguide, and optical fiber. The micrograph is of the nanowire on top of the waveguide, illuminated by an external halogen lamp. Figure 5d shows scattering from the ends of the nanowires when light from the optical fiber coupled into the waveguide. The effect is similar to that observed by Pyayt *et al.*, who found scattering from randomly deposited Ag

nanowires coupled to SU-8 waveguides.[43] The ease of integrating these single-crystalline nanowires with microfabricated dielectric waveguides, along with the observation of scattering from the ends of the nanowires, suggests that the wires could be used as plasmonic waveguides in a nanophotonic device.[44]

CONCLUSIONS

The combination of nanoskiving and magnetic mooring is useful for the assembly of nanostructures for simple, multicomponent electronic or optical devices. The technique is complementary to existing techniques for positioning and orienting nanostructures. Optical tweezing, for example, has control over individual structures with high accuracy, but is unable to control groups of structures and relies on a liquid medium. Methods of fluid-assisted alignment can align nanowires over large areas, but do not provide control over individual structures. Integrated fabrication and positioning is not provided by any other nonlithographic method.

Magnetic mooring is not limited to structures that can be produced by nanoskiving; any delicate film that contains ferromagnetic particles could be
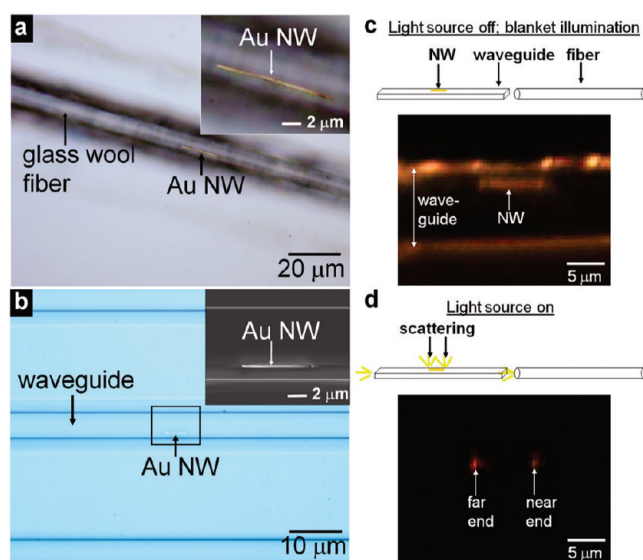
Figure 5. Optical micrographs of single-crystalline nanowires positioned on top of topographic features. (a) A nanowire (l = 15 μm, w = 150 nm, h = 100 nm) lying on the side of a fiber of glass wool. The inset is a magnified view of the same image. **(b)** A nanowire (l = 8 μm, w = 290 nm, h = 100 nm) placed on top of a polymeric optical waveguide microfabricated in SU-8 photoresist. The inset is an SEM image of the nanowire on top of the waveguide. **(c)** Schematic illustration and optical micrograph of the nanowire from panel b on the microfabricated waveguide. The image was obtained under external illumination from a halogen light source. **(d)** Schematic illustration and optical micrograph of the nanowire obtained by coupling light into the waveguide using an optical fiber. The only light visible was that which scattered from the ends of the nanowire.

positioned. Nanoskiving is, however, a convenient way of making such films. Any of the structures that have been fabricated using nanoskiving could be positioned and oriented by magnetic mooring. The presence of the epoxy slab preserves the spatial relationship between structures within each slab, a characteristic that could lead to more complex arrangements of nanostructures than those demonstrated. Stacking of 2D arrays of plasmonic resonators, for example, could provide a new route toward the fabrication of 3D metamaterials.[1]

Crossbar structures of metallic nanowires with a sub-micrometer pitch could be valuable for a variety of applications, including memory devices, tunnel diodes, and optical antennae.[45] Square arrays of conjugated polymer nanowires could be useful as high-surface-area organic semiconductors in heterojunction photodetectors, for example.[46] We believe that our process is particularly useful for assembling structures for nanophotonic applications. We showed that it was possible to position Au nanowires on glass fibers and photoresist features; these structures can serve as optical waveguides for photonic circuits, while single-crystalline metallic nanowires can serve as sub-λ plasmonic waveguides. Arrangements of these components in arbitrary geometries could enable the fabrication of nanophotonic devices comprising metallic nanowires,[47] semiconducting nanowires,[48] optical waveguides,[43] and single-photon emitters[4] or the fabrication of apertureless near-field optical probes.[44]

The most important limitations of magnetic mooring are the average positional deviation (16 μm) and the serial nature of depositing polymeric slabs one-by-one. We do not believe that we have achieved the highest accuracy possible for this technique. A combination of (i) increasing the strength of interaction between the slabs and the external magnets for faster correction of the errors caused by abrupt dewetting of the substrate as the drop edge approaches the floating slab, (ii) controlling the wettability of the substrates or the surface tension of the pool of liquid, or (iii) designing topographic features that dock the slabs before the receding edge of the drop of water influences their positions could increase the accuracy of positioning. An ideal apparatus would include dark-field optics, a camera, and a closed-loop system with a piezoelectronically controlled manipulator.[15] In the long term, magnetic interactions between thin polymeric slabs and external magnets (or between the slabs themselves) might be amenable to programmed or templated self-assembly.

METHODS

Fabrication of Au Nanowires Coembedded with Ni Strips (Figures 1 and 2a−e). We began by puddle casting an epoxy prepolymer (Epo-Fix, obtained from Electron Microscopy Sciences) against a test-grade Si wafer bearing no surface treatment. We generally used a ring of PDMS to contain the epoxy prepolymer. Thermal curing of the epoxy at 60 °C for 2 h, cooling to room temperature (rt), and separation of the cured epoxy from the Si template provided a smooth epoxy surface (rms roughness = 0.5 nm by atomic force microscopy). We coated this epoxy substrate with an 80-nm-thick film of Au by e-beam evaporation at a rate of 1−5 Å s^{-1}. We coated a second epoxy substrate with a 2-μm-thick film of Ni by e-beam evaporation at a rate of ∼10 Å s^{-1}. This film displayed buckling that did not adversely affect subsequent steps of the process. We cut the Au and Ni films on their epoxy substrates into strips (l ≈ 5 mm, w ≈ 300 μm) using a razor blade and a hammer. We placed Au and Ni strips face-to-face and embedded them in more epoxy (the two films were separated by

epoxy, not air). After curing, we placed this roughly embedded structure into a 1-mL polyethylene centrifuge tube and embedded it in additional epoxy. This action provided a block that could be secured in the ultramicrotome for sectioning. We exposed the cross section of the Au and Ni films using a jeweler's saw and trimmed the block facet into a rectangle with sides of 200−500 μm. We used an ultramicrotome (Leica Ultracut UCT) equipped with a 35° diamond knife (Diatome Ultra 35 with 1.8 or 2.4 mm length cutting edge) set to a clearance angle of 6°. All sections were collected at ambient temperature on the surface of deionized water (see the Supporting Information of Xu *et al.*[49] for a detailed description of the operation of the ultramicrotome). After sectioning, the slabs floated on the surface of a water-filled trough, were collected by hand using the Pefect Loop tool (Electron Microscopy Sciences), and were transferred to the substrate. The droplet of water spread into a pool with a diameter of ∼1 cm. At this point, we either placed the substrate in the apparatus for magnetic mooring or allowed the water to evaporate. Following deposition, optional etches of the epoxy

(SPI Plasma Prep II benchtop etcher, 100 W, 1 Torr ambient air, 15 min) and/or the Ni (Nickel Etchant, type TFB, Transene Company, Inc., etch rate 3 nm s^{-1} at 25 °C) generated free-standing nanowires.

Fabrication of Parallel Au Nanowires (Figures 2c−f, 3b, and 4b,c). We generated multiple parallel nanowires of Au in the same epoxy slab by sectioning parallel films of Au. We laminated multiple Au films together by evaporating an Au film on a flat epoxy substrate, applying a drop of epoxy prepolymer to the film, and curing it under compression by a flat slab of PDMS. The PDMS slab was pressed into the epoxy prepolymer by gravity or with a binder clip. After thermal curing of the epoxy, the substrate could again be coated with Au. This process could be repeated to form several parallel films. We cut this film into strips, embedded it with a Ni film or powder, trimmed the block, and sectioned it, as before.

Fabrication of Parallel Pd Nanowires (Figures 2f and 4c). We formed epoxy blocks containing multiple parallel films of Pd separated by thin epoxy layers by iterative stripping of an evaporated film of Pd (60 nm) off of a Si wafer. We placed a drop of epoxy prepolymer onto the surface of the Pd film. We placed a cured piece of epoxy of the same type against the drop of prepolymer, applied pressure with two binder clips, and thermally cured the epoxy in an oven at 200 °C for 15 min. After cooling for 5 min, release of the epoxy support transferred a region of the Pd film to the epoxy substrate. We extruded a second drop of epoxy on the wafer and again placed the support in contact with it, under pressure. Repetition of these steps provided a laminated structure with five layers of Pd separated by four layers of epoxy. We cut the laminated structure into strips with a razor blade, embedded a strip in additional epoxy prepolymer to form a block, and sectioned the block with the ultramicrotome. Etching in an air plasma removed the epoxy matrix and liberated five free-standing nanowires. The spacing between the wires was controlled by the pressure on the epoxy support and the viscosity of the epoxy prepolymer (initial viscosity = 0.05 Pa s). We were able to achieve a minimum spacing between nanowires of 70 nm.

Fabrication of P3HT Nanowires (Figure 3b). We synthesized regioregular P3HT using the McCullough method of polymerization.[42] We dissolved this material in chloroform at a concentration of 17 mg mL^{-1} and spin-coated it on a flat epoxy substrate at 1 krpm. Thermal annealing and removal of the solvent at 125 °C in a vacuum oven for 30 min produced a red film with a metallic luster. We cut the film into strips, embedded it with a Ni film or powder, trimmed the block, and sectioned it, as before.

Fabrication of Single-Crystalline Au Nanowires by Nanoskiving Chemically Synthesized Microplates. We described the fabrication of the single-crystalline nanowires in a previous report from our laboratory.[37] Briefly, we generated single crystalline microplates by heating a solution of HAuCl$_4$ in the presence of poly(vinylpyrrolidone) in ethylene glycol. We deposited microplates grown by this method onto flat epoxy substrates. We cut the substrates bearing Au microplates into strips, embedded it with a Ni film or powder, trimmed the block, and sectioned it, as before.

Fabrication of BBL Nanowires (Figure 4d). We fabricated groups of 50 parallel BBL nanowires using a previously published procedure.[34] Briefly, 100 total layers of BBL and a sacrificial polymer were spin-coated onto a glass slide, embedded in epoxy, and sectioned with the ultramicrotome. Etching with an air plasma removed the epoxy matrix and the sacrificial polymer. This process generated 50 parallel, free-standing BBL nanowires.

Apparatus for Magnetic Mooring. The apparatus for the process of positioning nanostructures embedded in thin films was constructed on a floating (antivibration) optical table (see Supporting Information for photographs of the apparatus). We used a stereomicroscope under 95× magnification, mounted on a boom stand, to monitor all positioning. Beneath the objective we mounted two stages to the optical table. All optical equipment was obtained from ThorLabs. The lower stage was equipped with the micromanipulators used for translation (PT1 translation stages for *x* and *y*) and rotation (PR01 high precision rotation mount for θ) of the magnets, which were two parallel columns of three cylindrical permanent magnets (*d* = 0.125 in., *l* = 0.375 in., grade N42, NdFeB) with the polarization of each col-

umn pointing in opposite directions. The upper stage was an aluminum slab (MB6 aluminum breadboard, 6 in. × 6 in. × 0.5 in.) containing a circular hole (*d* = 1.5 in.) on top of which the typical substrate, a Si wafer (*d* = 2 or 3 in.), sat. The upper stage was brought down toward the lower stage such that the column of magnets sat <0.5 mm from the bottom of the Si wafer, through the hole in the upper stage. The maximum values of magnetic field in the transverse direction were 2.2 kG and −2.2 kG, above the centers of the magnets in the plane of the substrate, as determined by a Gauss meter. The substrate and upper stage were heated to 36 °C to quicken the evaporation of water using a halogen lamp placed ~10 cm from the stage. The substrate was covered by a Petri dish cover to protect the floating slabs from disturbances by air currents in the room. Holes drilled into the Petri dish cover with a heated syringe needle allowed water vapor to escape.

Imaging. Optical imaging (Figures 2 and 5) was performed using an upright optical microscope (Leica DMRX). Scanning electron microscope (SEM) images (Figures 3, 4, and 5b) of the epoxy sections were acquired with a Zeiss Ultra55 or Supra55 VP field-emission SEM at 5 kV with a working distance of 2−6 mm.

Coupling of Light into Au Nanowires Using Polymeric Waveguides (Figure 5b−d). We fabricated waveguides of SU-8 2002 negative resist on a Si wafer bearing 3 μm of SiO$_2$ using e-beam lithography at 100 kV (Elionix 7000). We moored a single-crystalline nanowire on top of the polymeric waveguide; we did not etch the epoxy matrix nor the Ni strip as they did not interfere with the observation of scattering from the termini of the nanowires. Light from a supercontinuum source (Koheras) was coupled to the waveguide using a tapered lensed fiber (Nanonics Inc.).

Supporting Information Available: Photographs of the apparatus used for magnetic micromooring and images of nanowires from which the positional and rotational accuracy of the technique was calculated. This material is available free of charge *via* the Internet at http://pubs.acs.org.

REFERENCES AND NOTES

1. Xu, Q.; Rioux, R. M.; Whitesides, G. M. Fabrication of Complex Metallic Nanostructures by Nanoskiving. *ACS Nano* **2007**, *1*, 215–227.

2. Xu, Q. B.; Rioux, R. M.; Dickey, M. D.; Whitesides, G. M. Nanoskiving: A New Method To Produce Arrays of Nanostructures. *Acc. Chem. Res.* **2008**, *41*, 1566–1577.

3. Xia, Y. N.; Yang, P. D.; Sun, Y. G.; Wu, Y. Y.; Mayers, B.; Gates, B.; Yin, Y. D.; Kim, F.; Yan, Y. Q. One-Dimensional Nanostructures: Synthesis, Characterization, and Applications. *Adv. Mater.* **2003**, *15*, 353–389.

4. Akimov, A. V.; Mukherjee, A.; Yu, C. L.; Chang, D. E.; Zibrov, A. S.; Hemmer, P. R.; Park, H.; Lukin, M. D. Generation of Single Optical Plasmons in Metallic Nanowires Coupled to Quantum Dots. *Nature* **2007**, *450*, 402–406.

5. Cao, Q.; Rogers, J. A. Ultrathin Films of Single-Walled Carbon Nanotubes for Electronics and Sensors: A Review of Fundamental and Applied Aspects. *Adv. Mater.* **2009**, *21*, 29–53.

6. Heo, K.; Kim, C. J.; Jo, M. H.; Hong, S. Massive Integration of Inorganic Nanowire-Based Structures on Solid Substrates for Device Applications. *J. Mater. Chem.* **2009**, *19*, 901–908.

7. Stover, C. A.; Koch, D. L.; Cohen, C. Observations of Fiber Orientation in Simple Shear-Flow of Semidilute Suspensions. *J. Fluid Mech.* **1992**, *238*, 277–296.

8. Zhong, Z. H.; Wang, D. L.; Cui, Y.; Bockrath, M. W.; Lieber, C. M. Nanowire Crossbar Arrays as Address Decoders for Integrated Nanosystems. *Science* **2003**, *302*, 1377–1379.

9. Cui, Y.; Lieber, C. M. Functional Nanoscale Electronic Devices Assembled Using Silicon Nanowire Building Blocks. *Science* **2001**, *291*, 851–853.

10. Huang, Y.; Duan, X. F.; Wei, Q. Q.; Lieber, C. M. Directed Assembly of One-Dimensional Nanostructures into Functional Networks. *Science* **2001**, *291*, 630–633.

11. Messer, B.; Song, J. H.; Yang, P. D. Microchannel Networks for Nanowire Patterning. *J. Am. Chem. Soc.* **2000**, *122*, 10232–10233.

12. Yu, G. H.; Cao, A. Y.; Lieber, C. M. Large-Area Blown Bubble Films of Aligned Nanowires and Carbon Nanotubes. *Nat. Nanotechnol.* **2007**, *2*, 372–377.

13. Fan, Z. Y.; Ho, J. C.; Jacobson, Z. A.; Yerushalmi, R.; Alley, R. L.; Razavi, H.; Javey, A. Wafer-Scale Assembly of Highly Ordered Semiconductor Nanowire Arrays by Contact Printing. *Nano Lett.* **2008**, *8*, 20–25.

14. Jin, S.; Whang, D. M.; McAlpine, M. C.; Friedman, R. S.; Wu, Y.; Lieber, C. M. Scalable Interconnection and Integration of Nanowire Devices without Registration. *Nano Lett.* **2004**, *4*, 915–919.

15. Pauzauskie, P. J.; Radenovic, A.; Trepagnier, E.; Shroff, H.; Yang, P. D.; Liphardt, J. Optical Trapping and Integration of Semiconductor Nanowire Assemblies in Water. *Nat. Mater.* **2006**, *5*, 97–101.

16. Jamshidi, A.; Pauzauskie, P. J.; Schuck, P. J.; Ohta, A. T.; Chiou, P. Y.; Chou, J.; Yang, P. D.; Wu, M. C. Dynamic Manipulation and Separation of Individual Semi-conducting and Metallic Nanowires. *Nat. Photonics* **2008**, *2*, 85–89.

17. Postma, H. W. C.; Sellmeijer, A.; Dekker, C. Manipulation and Imaging of Individual Single-Walled Carbon Nanotubes with an Atomic Force Microscope. *Adv. Mater.* **2000**, *12*, 1299–1302.

18. Sirbuly, D. J.; Law, M.; Pauzauskie, P.; Yan, H. Q.; Maslov, A. V.; Knutsen, K.; Ning, C. Z.; Saykally, R. J.; Yang, P. D. Optical Routing and Sensing with Nanowire Assemblies. *Proc. Natl. Acad. Sci. U.S.A.* **2005**, *102*, 7800–7805.

19. Smith, P. A.; Nordquist, C. D.; Jackson, T. N.; Mayer, T. S.; Martin, B. R.; Mbindyo, J.; Mallouk, T. E. Electric-Field Assisted Assembly and Alignment of Metallic Nanowires. *Appl. Phys. Lett.* **2000**, *77*, 1399–1401.

20. Yun, M. H.; Myung, N. V.; Vasquez, R. P.; Lee, C. S.; Menke, E.; Penner, R. M. Electrochemically Grown Wires for Individually Addressable Sensor Arrays. *Nano Lett.* **2004**, *4*, 419–422.

21. Chai, J.; Buriak, J. M. Using Cylindrical Domains of Block Copolymers to Self-Assemble and Align Metallic Nanowires. *ACS Nano* **2008**, *2*, 489–501.

22. Tanase, M.; Silevitch, D. M.; Hultgren, A.; Bauer, L. A.; Searson, P. C.; Meyer, G. J.; Reich, D. H. Magnetic Trapping and Self-Assembly of Multicomponent Nanowires. *J. Appl. Phys.* **2002**, *91*, 8549–8551.

23. Tanase, M.; Bauer, L. A.; Hultgren, A.; Silevitch, D. M.; Sun, L.; Reich, D. H.; Searson, P. C.; Meyer, G. J. Magnetic Alignment of Fluorescent Nanowires. *Nano Lett.* **2001**, *1*, 155–158.

24. Love, J. C.; Urbach, A. R.; Prentiss, M. G.; Whitesides, G. M. Three-Dimensional Self-Assembly of Metallic Rods with Submicron Diameters Using Magnetic Interactions. *J. Am. Chem. Soc.* **2003**, *125*, 12696–12697.

25. Zhang, S.; Zhu, H. Y.; Hu, Z. B.; Liu, L.; Chen, S. F.; Yu, S. H. Multifunctional Necklace-Like Cu@Cross-Linked Poly(vinyl alcohol) Microcables with Fluorescent Property and Their Manipulation by an External Magnet. *Chem. Commun.* **2009**, 2326–2328.

26. Hangarter, C. M.; Myung, N. V. Magnetic Alignment of Nanowires. *Chem. Mater.* **2005**, *17*, 1320–1324.

27. Fu, A. H.; Hu, W.; Xu, L.; Wilson, R. J.; Yu, H.; Osterfeld, S. J.; Gambhir, S. S.; Wang, S. X. Protein-Functionalized Synthetic Antiferromagnetic Nanoparticles for Biomolecule Detection and Magnetic Manipulation. *Angew. Chem., Int. Ed.* **2009**, *48*, 1620–1624.

28. Platt, M.; Muthukrishnan, G.; Hancock, W. O.; Williams, M. E. Millimeter Scale Alignment of Magnetic Nanoparticle Functionalized Microtubules in Magnetic Fields. *J. Am. Chem. Soc.* **2005**, *127*, 15686–15687.

29. Fung, A. O.; Kapadia, V.; Pierstorff, E.; Ho, D.; Chen, Y. Induction of Cell Death by Magnetic Actuation of Nickel Nanowires Internalized by Fibroblasts. *J. Phys. Chem. C* **2008**, *112*, 15085–15088.

30. Liong, M.; Lu, J.; Kovochich, M.; Xia, T.; Ruehm, S. G.; Nel, A. E.; Tamanoi, F.; Zink, J. I. Multifunctional Inorganic Nanoparticles for Imaging, Targeting, and Drug Delivery. *ACS Nano* **2008**, *2*, 889–896.

31. Yellen, B. B.; Hovorka, O.; Friedman, G. Arranging Matter by Magnetic Nanoparticle Assemblers. *Proc. Natl. Acad. Sci. U.S.A.* **2005**, *102*, 8860–8864.

32. Lapointe, C. P.; Reich, D. H.; Leheny, R. L. Manipulation and Organization of Ferromagnetic Nanowires by Patterned Nematic Liquid Crystals. *Langmuir* **2008**, *24*, 11175–11181.

33. Shi, F.; Liu, S. H.; Gao, H. T.; Ding, N.; Dong, L. J.; Tremel, W.; Knoll, W. Magnetic-Field-Induced Locomotion of Glass Fibers on Water Surfaces: Towards the Understanding of How Much Force One Magnetic Nanoparticle Can Deliver. *Adv. Mater.* **2009**, *21*, 1927–1930.

34. Lipomi, D. J.; Chiechi, R. C.; Dickey, M. D.; Whitesides, G. M. Fabrication of Conjugated Polymer Nanowires by Edge Lithography. *Nano Lett.* **2008**, *8*, 2100–2105.

35. Lipomi, D. J.; Chiechi, R. C.; Reus, W. F.; Whitesides, G. M. Laterally Ordered Bulk Heterojunction of Conjugated Polymers: Nanoskiving a Jelly Roll. *Adv. Funct. Mater.* **2008**, *18*, 3469–3477.

36. Xu, Q. B.; Gates, B. D.; Whitesides, G. M. Fabrication of Metal Structures with Nanometer-Scale Lateral Dimensions by Sectioning Using a Microtome. *J. Am. Chem. Soc.* **2004**, *126*, 1332–1333.

37. Wiley, B. J.; Lipomi, D. J.; Bao, J. M.; Capasso, F.; Whitesides, G. M. Fabrication of Surface Plasmon Resonators by Nanoskiving Single-Crystalline Gold Microplates. *Nano Lett.* **2008**, *8*, 3023–3028.

38. O'Handley, R. C. *Modern Magnetic Materials: Principles and Applications*; Wiley: New York, 2000; pp 42−43.

39. Liu, H. Q.; Kameoka, J.; Czaplewski, D. A.; Craighead, H. G. Polymeric Nanowire Chemical Sensor. *Nano Lett.* **2004**, *4*, 671–675.

40. Liu, H. Q.; Reccius, C. H.; Craighead, H. G. Single Electrospun Regioregular Poly(3-hexylthiophene) Nanofiber Field-Effect Transistor. *Appl. Phys. Lett.* **2005**, *87*, 253106-1–253106-3.

41. Loewe, R. S.; Ewbank, P. C.; Liu, J. S.; Zhai, L.; McCullough, R. D. Regioregular, Head-to-Tail Coupled Poly(3-alkylthiophenes) Made Easy by the GRIM Method: Investigation of the Reaction and the Origin of Regioselectivity. *Macromolecules* **2001**, *34*, 4324–4333.

42. McCullough, R. D. The Chemistry of Conducting Polythiophenes. *Adv. Mater.* **1998**, *10*, 93–116.

43. Pyayt, A. L.; Wiley, B.; Xia, Y. N.; Chen, A.; Dalton, L. Integration of Photonic and Silver Nanowire Plasmonic Waveguides. *Nat. Nanotechnol.* **2008**, *3*, 660–665.

44. Prasad, P. N. *Nanophotonics*; John Wiley & Sons, Inc.: Hoboken, NJ, 2005; pp 62−65.

45. Berland, B. Photovoltaic Technologies Beyond the Horizon: Optical Rectenna Solar Cell; Subcontractor Report for National Renewable Energy Laboratory, 2003.

46. Yang, F.; Shtein, M.; Forrest, S. R. Controlled Growth of a Molecular Bulk Heterojunction Photovoltaic Cell. *Nat. Mater.* **2005**, *4*, 37–41.

47. Ditlbacher, H.; Hohenau, A.; Wagner, D.; Kreibig, U.; Rogers, M.; Hofer, F.; Aussenegg, F. R.; Krenn, J. R. Silver Nanowires as Surface Plasmon Resonators. *Phys. Rev. Lett.* **2005**, *95*, 257403-1–257403-4.

ARTICLE

48. Falk, A. L.; Koppens, F. H. L.; Yu, C. L.; Kang, K.; Snapp, N. D.; Akimov, A. V.; Jo, M. H.; Lukin, M. D.; Park, H. Near-Field Electrical Detection of Optical Plasmons and Single Plasmon Sources. *Nat. Phys.* **2009**, *5*, 475–479.

49. Xu, Q. B.; Bao, J. M.; Rioux, R. M.; Perez-Castillejos, R.; Capasso, F.; Whitesides, G. M. Fabrication of Large-Area Patterned Nanostructures for Optical Applications by Nanoskiving. *Nano Lett.* **2007**, *7*, 2800–2805.

ARTICLE